# Rheological Profiling of Organogels Prepared at Critical Gelling Concentrations of Natural Waxes in a Triacylglycerol Solvent

Ashok R. Patel,*,[†] Mehrnoosh Babaahmadi,[†] Ans Lesaffer,[‡] and Koen Dewettinck[†]

[†]Vandemoortele Centre for Lipid Science and Technology, Laboratory of Food Technology and Engineering, Faculty of Bioscience Engineering, Ghent University, Coupure Links 653, 9000 Gent, Belgium

[‡]Vandemoortele R &D Izegem, Prins Albertlaan 79, 8870 Izegem, Belgium

Ⓢ Supporting Information

**ABSTRACT:** The aim of this study was to use a detailed rheological characterization to gain new insights into the gelation behavior of natural waxes. To make a comprehensive case, six natural waxes (differing in the relative proportion of chemical components: hydrocarbons, fatty alcohols, fatty acids, and wax esters) were selected as organogelators to gel high-oleic sunflower oil. Flow and dynamic rheological properties of organogels prepared at critical gelling concentrations ($C_g$) of waxes were studied and compared using drag (stress ramp and steady flow) and oscillatory shear (stress and frequency sweeps) tests. Although, none of the organogels satisfied the rheological definition of a "strong gel" ($G''/G'$ ($\omega$) $\leq 0.1$), on comparing the samples, the strongest gel (highest critical stress and dynamic, apparent, and static yield stresses) was obtained not with wax containing the highest proportion of wax esters alone (sunflower wax, SFW) but with wax containing wax esters along with a higher proportion of fatty alcohols (carnauba wax, CRW) although at a comparatively higher $C_g$ (4%wt for latter compared to 0.5%wt for former). As expected, gel formation by waxes containing a high proportion of lower melting fatty acids (berry, BW, and fruit wax, FW) required a comparatively higher $C_g$ (6 and 7%wt, respectively), and in addition, these gels showed the lowest values for plateau elastic modulus ($G'_{LVR}$) and a prominent crossover point at higher frequency. The gelation temperatures ($T_{G'=G''}$) for all the studied gels were lower than room temperature, except for SFW and CRW. The yielding-type behavior of gels was evident, with most gels showing strong shear sensitivity and a weak thixotropic recovery. The rheological behavior was combined with the results of thermal analysis and microstructure studies (optical, polarized, and cryo-scanning electron microscopy) to explain the gelation properties of these waxes.

**KEYWORDS:** organogels, natural waxes, rheological characterization, cryo-SEM, microstructure, wax-based gels

## ■ INTRODUCTION

Organogels are a class of soft matter systems that are considered to be at an interface of complex fluids and phase-separated states of matter. They comprise an organic liquid that is physically immobilized by a network of dispersed, self-assembled aggregates of gelator molecules.[1,2] The normal phase separation into aggregated gelator molecules and liquid solvent phase is avoided in organogels due to the organization of aggregated gelator molecules into an interconnected solid-like, three-dimensional (3D) network, resulting in the formation of strong or weak gels depending on the gelator–gelator interactions as well as the solvent properties.[1,3,4] The possibility of transforming different types of organic liquids into solid-like viscoelastic gels (at relatively lower mass fractions of gelator molecules) makes organogelation an attractive subject of investigation in varied research domains for many different applications. For example, systems where triacylglycerol solvents (vegetable oils) are gelled using natural components, have found potential applications in biorelated fields such as drug delivery,[5–7] cosmetics,[8–10] and foods.[11–13] Among various gelators explored for gelling vegetable oils, natural waxes are considered to be the most promising ones because of their excellent oil binding properties,[14] economical value (capable of gelling oils at a significantly lower mass fractions, $w_c \ll 0.1$),[15,16] and availability of a number of waxes approved for use in humans.[17,18] Moreover, the gels formed using waxes have

interesting properties such as themoreversibility[19,20] and emulsion stabilization,[21–23] which further justifies their popularity as organogelators for vegetable oils.

In spite of such widespread interest in these systems, a clear fundamental understanding of the physical properties of wax-based organogels is still missing. Unlike other low molecular weight gelators, waxes have a multicomponent chemical nature, comprising of components such as hydrocarbons (HCs), wax esters (WEs), fatty acids (FAs), and fatty alcohols (FALs), and such chemical diversity makes characterization of wax-based organogels very complicated. Some fundamental studies have been published in recent years where the gelation behavior of waxes was explored based on the chemical properties of waxes (composition, impurities),[15] thermodynamics and kinetic aspects of wax crystallization (fractal aggregation, thermal properties, crystal morphology, and cooling rates),[14,24,25] and some rheological[26–28] and large deformation studies (texture analysis) of the formed gels.[20] As seen with fats (high-melting triacylglycerols, TAGs), waxes also crystallize in low-melting TAGs (liquid oil) when the temperature is decreased well below their melting temperatures. Fundamentally, this type of

A

crystallization includes characteristics of both melt crystallization (crystallization due to supercooling) and crystallization of solute from the solvent (crystallization due to the decreased solubility of waxes in oils at lower temperatures). Similar to fat crystallization, the formed crystallites of waxes undergo further thermodynamically induced structural reorganization including clustering and aggregation. These crystalline aggregates can act as building blocks to trap the liquid oil into a gel-like structure, resulting in organogel formation. The structure is stabilized via weak interactions (among the neighboring building blocks) such as H-bonding and polar−polar interactions among constituents with polar moieties as well as weak intermolecular interactions such as induced dipole−induced dipole interactions (London dispersion force) among nonpolar components.

In our opinion, there is a need for a comprehensive comparative rheological profiling of wax-based organogels in order to further probe the link between the macroscopic flow/deformation response of gels and the microscopic interactions between the constituent building blocks (crystalline aggregates). In the present study, we report a detailed rheological characterization using a range of steady and dynamic shear measurements to understand the gelation behavior of natural waxes. To make a comprehensive case, six natural waxes (differing in the relative proportion of chemical components: HCs, WEs, FAs, and FALs) were selected to prepare organogels using high-oleic sunflower oil as the triacylglycerol solvent. The critical gelling concentrations ($C_g$) for different waxes were identified, and the flow and dynamic rheological properties of organogels prepared at $C_g$ of waxes were studied and compared using drag (stress ramp), steady flow (flow and 3ITT (3 interval thixotropy test)), oscillatory shear (stress and frequency sweeps), and mixed flow−oscillatory shear tests. The results obtained from these measurements were combined with the results from thermal behavior and microstructure studies to characterize the physical properties of organogels. The $C_g$ is the minimum concentration of wax at which the gelation of solvent occurs, and since we are considering wax-based organogels as fractal gels, the $C_g$ in this case corresponds to the minimum volume fraction of crystalline particles at which a space-filling network of rarefied fractal flocs is formed.[29] Below this concentration, the dispersed particles contribute only in increasing the viscosity of the sol, whereas at concentrations higher than $C_g$ a decrease in the size of fractal flocs is observed with a resultant increase in fractal dimensions due to the densification of flocs.[30] Thus, the viscoelasticity of fractal gels is best studied at $C_g$ in order to better understand the nature of molecular interactions involved in gel formation at low volume fractions of particles.

## ■ MATERIALS AND METHODS

**Materials.** Refined high-oleic sunflower oil, HOS (TAGs > 99% wt), was received from Vandemoortele Lipids N.V. (Izegem, Belgium). Sunflower wax, *Helianthus Annuus Seed Cera* (SFW, acid value: 2−8 mg KOH/g, saponification value: 75−95 mg KOH/g), carnauba wax, *Copernicia Cerifera Cera* (CRW, acid value: 2−7 mg KOH/g, saponification value: 78−95 mgKOH/g), candelilla wax, *Euphorbia Cerifera Cera* (CLW, acid value: 12−22 mg KOH/g, saponification value: 43−65 mgKOH/g), bees wax, *Cera Alba* (BZW, acid value: 17−22 mg KOH/g, saponification value: 70−80 mgKOH/g), berry wax, *Rhus Verniciflua Peel Cera* (BW, acid value: 48−54 mg KOH/g, saponification value: 180−220 mgKOH/g), and fruit wax, *Myrica Cerifera* (FW, acid value: 5−25 mg KOH/g, saponification value: 210−240 mgKOH/g) were received as gift samples from Kalh GmbH &

Co. KG (Trittau, Germany). Chemical composition of waxes was determined in-house using HPLC-ELSD to understand the distribution of main components. The main components of six waxes are listed in Table S1. More details on the experimental setup and result analysis will be published elsewhere.

**Preparation of Organogels.** Waxes were dispersed in HOS at varying concentrations by heating above their melting points until complete melting of waxes was achieved. The clear oily dispersions were subsequently cooled to 5 °C at a rate of approximately 2 °C/min under mild stirring (200 rpm) using a magnetic stirrer (model EM3300T, Labotech Inc., Germany). The critical gelling concentration ($C_g$) for all six waxes was identified using rheological characterization (oscillatory frequency sweeps). Samples prepared at different concentrations of waxes were subject to frequency sweeps at a constant stress of 0.02 Pa. The resultant values of elastic and viscous modulus ($G'$ and $G''$, respectively) were compared at low frequency, and the corresponding concentrations at which $G' > G''$ were identified as $C_g$ for individual waxes. The samples were stored at 5 °C until used further for characterization. The photograph of gels prepared at the respective $C_g$ of waxes is shown in Figure S1.

**Thermal Characterization.** The thermal behavior of neat waxes and wax-based organogels was determined in triplicate using a Q1000 DSC (TA Instruments, New Castle, DE, USA) equipped with a refrigerated cooling system. Nitrogen was used as purge gas. The cell constant and temperature were set with indium (TA Instruments). An additional temperature calibration was done using azobenzene (Sigma-Aldrich, Bornem, Belgium) and undecane (Acros Organics, Geel, Belgium). The wax samples were heated at 90 °C in sealed aluminum pans (TA Instruments) before being cooled to 0 °C, kept isothermally at 0 °C for 20 min, and reheated to 90 °C. Heating and cooling were done at a constant rate of 2 °C/min. Characteristic parameters of the thermal curves, including onset and peak maximum temperatures for crystallization and melting ($T_c$ onset, $T_m$ onset, $T_c$ peak, and $T_m$ peak), were obtained using the software TA Universal Analysis provided by the instrument supplier.

**Microstructure Studies.** The microstructure of wax crystals was observed under normal and polarized light (PLM) using a Leica DM2500 microscope (Wetzlar, Germany) equipped with a Leica MC170 HD color camera. For cryo-scanning electron microscopy (cryo-SEM), deoiling of organogel samples was carried out using butanol to remove the surface liquid oil in order to visualize the wax crystals. Precisely, the deoiling was carried out in two different ways: (1) A known quantity of organogel was weighed in a glass vial followed by addition of butanol (at a gel:butanol ratio of 1:50 w/w approximately), which led to the collapse of the gel structure and resultant sedimentation of the crystalline fraction. After overnight storage, the supernatant liquid was decanted to collect the sediment, which was then placed on the sample holder. (2) The organogel sample was directly placed on a specialized stub (sample holder with grooves) followed by a dropwise addition of butanol to remove the liquid oil. The stub was left for overnight drying in inverted position to drain out all the solvent. The stub was then plunge-frozen in liquid nitrogen and transferred into the cryo-preparation chamber (PP3010T Cryo-SEM Preparation System, Quorum Technologies, UK), where it was freeze-fractured and subsequently sputter-coated with Pt and examined in a JEOL JSM 7100F SEM (JEOL Ltd., Tokyo, Japan).

**Rheological Measurements.** An advanced rheometer AR 2000ex (TA Instruments, USA) equipped with a Peltier system for temperature control was used for all rheological measurements. A parallel plate cross-hatched geometry of diameter 40 mm was used (geometry gap = 1000 μm) for the following tests: (a) amplitude sweeps: oscillatory stress = 0.001−1000 Pa, frequency = 1 Hz, and temperature = 5 °C; (b) frequency sweeps: oscillatory stress = 0.02 Pa, angular frequency = 0.6−240 rads⁻¹, and temperature = 5 °C; (c) temperature ramps: oscillatory stress = 0.02 Pa, frequency = 1 Hz, and temperature = 90−5 °C; (d) stress ramp: shear stress (0.08−300 Pa) and temperature = 5 °C; (e) flow-frequency test: samples were subjected to a range of shear rate = 0.01−20 s⁻¹ followed by frequency sweeps ($v$ = 0.01−10 Hz); and (f) 3-ITT: samples were subjected to alternating intervals of low and high shear rates (0.1 s⁻¹ for 10 min, 1
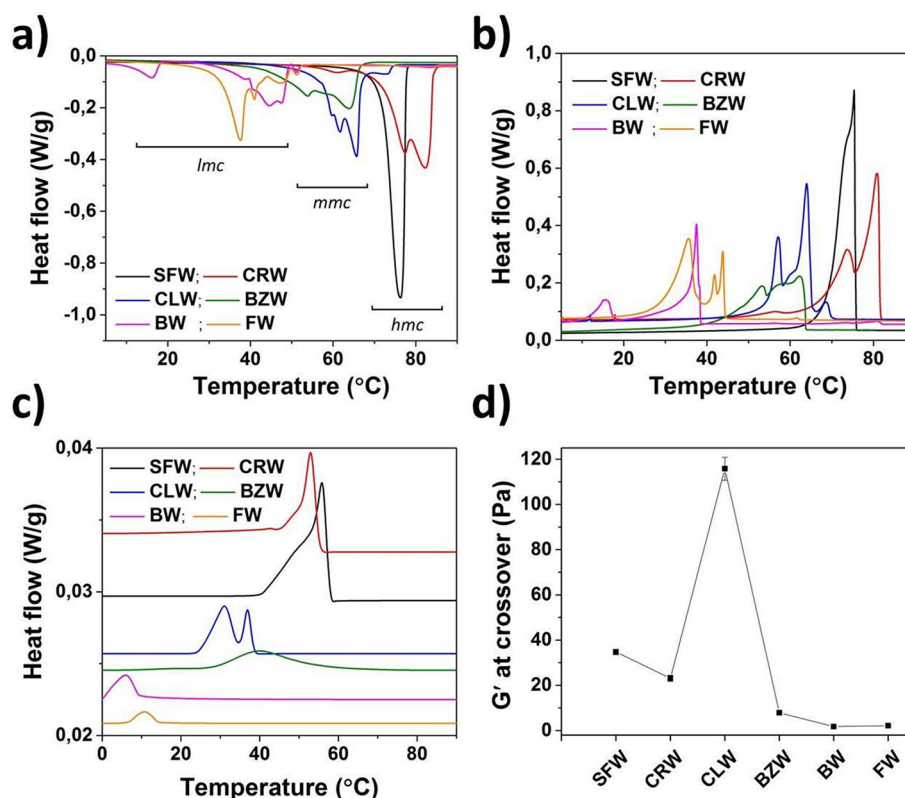
**Figure 1.** Comparative heating (a) and cooling (b) curves of neat waxes; (c) cooling curves of organogels prepared at the $C_g$ of respective waxes; and (d) elastic modulus ($G'$) at crossover point for organogels prepared at the $C_g$ of respective waxes (also refer to Figure S3).

$s^{-1}$ for next 5 min, followed by 0.1 $s^{-1}$ for 10 min) at a temperature of 5 °C. The apparent yield stress was measured by fitting the stress versus shear rate data to a three-parameter model (Hershel Bulkley model) as discussed later.

**Statistical Analysis.** Data from texture and sensorial evaluation of cakes were compared using statistical analysis. An unpaired, two-tailed Student's $t$ test was used on the data (SPSS Statistics) to establish the statistical significance in the differences observed.

## ■ RESULTS AND DISCUSSION

Waxes are a complex mixtures of a number of nonpolar and polar components with major components being HCs, WEs, FAs, and FALs with varying carbon chain lengths (representative molecular structures of main components are shown in Figure S2). When a liquid dispersion of a melted wax in an apolar solvent is cooled to temperatures well below the melting temperatures of wax (supercooling), the components separate out into crystalline phase that aggregate and further interconnect to form a 3D network that physically traps the liquid solvent into a gel structure.[31,32] Depending on the major component(s) as well as the carbon chain lengths of these components, the waxes display strikingly different gelation properties. The goal of this study was to have a detailed rheological profiling of wax-based physical gels in order to better understand their physical properties. To accomplish the goal, we selected six chemically diverse (differing in the proportions of major components) natural waxes: SFW, CRW, CLW, BZW, BW, and FW as listed in Table S1. DSC melting and cooling curves of neat waxes are shown in Figure 1a and b. On the basis of the melting peaks, the samples were categorized into waxes containing high-, mid-, and low-melting components (*hmc, mmc,* and *lmc,* respectively). SFW was predominantly rich (>95%wt) in WEs and showed single melting and crystal-

lization peaks and, hence, was considered as a monocomponent wax, while the other five waxes contained at least two chemical components in high proportions as follows: CRW (WEs, ∼62% wt; FALs, ∼30%wt), CLW (HCs, ∼73%wt; WEs, ∼16%wt; FAs, ∼9%wt), BZW (WEs, ∼58%wt; HCs, ∼27%wt; FAs, ∼9% wt); BW (FAs, ∼96%wt; FALs, ∼4%wt), and FW (FAs, ∼36% wt; FALs, ∼63%wt). Please note that some FAs in BW and FW are esterified to a glycerol backbone. The multicomponent nature of these waxes is further confirmed from multiple melting and crystallization peaks seen in Figure 1a and b.

To identify the critical gelling concentration (Table 1), a series of oily dispersions were made by varying the concentration of waxes, heating them at 90 °C, and subsequently cooling the dispersion to 5 °C at a constant rate of 2 °C/min. The gelation was noted first by simple tube flipping observation to identify the concentration ranges where the gels did not flow under the influence of gravity, followed by

**Table 1. Critical Gelling Concentration ($C_g$) and Crystallization Onset ($T_c$ Onset) and Peak ($T_c$ Peak) and Crossover ($T_{G'=G''}$) Temperatures (Mean ± SD) for Waxes in Organogels Prepared at Their Respective $C_g$**

| axis | $C_g$ (% wt) | $T_c$ onset (°C) | $T_c$ peak (°C) | $T_{G'=G''}$ (°C) |
|---|---|---|---|---|
| SFW | 0.5 | 57.27 ± 0.05 | 55.97 ± 0.31 | 45.9 ± 2.1 |
| CRW | 4 | 54.61 ± 0.05 | 52.83 ± 0.44 | 32.7 ± 1.3 |
| CLW | 0.75 | 38.72 ± 0.82 (I) | 37.76 ± 0.84 (I) | 13.1 ± 0.9 |
| | | 34.06 ± 0.12 (II) | 31.14 ± 0.42 (II) | |
| BZW | 1 | 42.69 ± 0.35 | 40.98 ± 0.75 | 19.0 ± 0.7 |
| BW | 6 | 8.92 ± 0.41 | 6.27 ± 0.03 | 7.3 ± 0.2 |
| FW | 7 | 14.87 ± 0.11 | 10.55 ± 0.07 | 17.3 ± 1.0 |

oscillatory rheological measurements (amplitude sweeps) to distinguish between a gel ($G' > G''$) and a viscous sol ($G'' > G'$) at low applied shear ($\tau_o$). Oscillatory measurements offer a convenient way of measuring the flow and deformation properties of viscoelastic samples and also facilitate the classification of samples into strong gels, weak gels, and viscous sols based on frequency sweeps.[33]

For viscoelastic materials, the frequency-dependent functions $G'$ and $G''$ give a measure of solid-like and liquid-like characteristics, respectively. Typically, for gels the elastic component ($G'$) dominates over the viscous component ($G''$) at small applied shear and attains a plateau ($G'_{LVR}$) in the linear response region (LVR, or linear viscoelastic region).[34] The end of the LVR is marked by the first point where the $G'$ varies by 10% of the $G'_{LVR}$ value, and the corresponding stress at this point is referred to as the critical stress ($\tau^*$). As the applied shear increases further, a permanent deformation (yielding) of the materials may occur ($G' = G''$), and the corresponding stress value at this point is referred to as oscillatory or dynamic yield stress ($\tau_{dy}$).[35] The $\tau^*$ represents the onset of nonlinearity (and hence structure breakdown), while $\tau_{dy}$ represents the transition from solid- to liquid-like behavior, and the zone spanning these two events is referred to as the yield zone.[36,37]

There is a significant discussion in the literature relating that the monocomponent gel formation in apolar solvents by low molecular weight gelators is usually achieved by a competitive interplay of fibrous structure formation and crystallization. The gelator—gelator interactions (mediated via hydrogen bonding, electron transfer, etc.) need to be anisotropic (unidirectional) to promote assembly into 1D fibers, and the relative absence of such interactions in the other two dimensions prevents lateral growth and subsequent crystallization.[38,39] The self-assembly gets more complicated when dealing with multicomponent systems; when more than one self-assembling components are present, they can either coassemble (heterogeneous assembly) or undergo "self-sorting" (coexisting, monomolecular assemblies) depending on the intermolecular interactions arising from similarities and dissimilarities in the chemical structures.[40] As the concentration of the gelator(s) exceeds a certain concentration ($C_g$), the equivalent spherical volumes of self-assembled linear aggregates (of anisotropically stacked gelator molecules) start overlapping and an interconnected 3D network is formed, leading to the formation of physical gels.[1,2] Such a behavior can be compared to the overlapping of hydrodynamic volumes of polymeric chains in semidilute solutions at a defined overlap concentration ($C^*$) that is specific for a polymer—solvent combination.[41]

As seen from Table 1, SFW, CLW, and BZW could form a gel at a significantly lower concentration ($C_g \leq 1\%wt$), whereas BW and FW required concentrations as high as 6 and 7%wt, respectively to gel the liquid oil. The higher $C_g$ values for BW and FW were expected since these waxes are devoid of components with a larger "carbon backbone"; they are mainly composed of low-melting short-chain FAs ($C_{14:0}$, $C_{16:0}$, $C_{18:0}$) and FALs ($C_{20-22}$). The relatively higher solubility of these components is also confirmed from the crystallization peaks of BW and FW organogels (Figure 1c), where the peaks are shifted to much lower temperatures compared to the peaks of neat waxes. To further understand the relationship between crystallization and gelation, a single frequency test was done on samples where the material functions ($G'$ and $G''$) were measured as a function of temperature (at constant $\tau = 0.02$ Pa

and $\nu = \omega/2\pi = 1$ Hz). The temperature ($T_{G'=G''}$) and $G'$ at the crossover point (or sol—gel transformation point) for organogel samples at $C_g$ of individual waxes are shown in Figure 1d. Interestingly, for waxes containing high- and mid-melting components, a prominent delay in gelation was evident with $T_{G'=G''}$ being much lower than $T_c$ peak (Table 1), while for BW and FW the gelation and crystallization occurred simultaneously. On comparing the $G'$ values for the gels at their respective crossover points, one can assume that the gelation of BW and FW gels ($G' < 2.5$ Pa) is not preceded by extensive microstructure development, in contrast to the gels formed by waxes containing high- and mid-melting components. In BW and FW, most FAs are not free but esterified to a glycerol backbone, and these nonlinear molecules display lateral packing leading to the formation of large crystals.

Due to the formation of relatively larger spherical crystal/crystalline aggregates (Figure 2a—f) by BW and FW (along
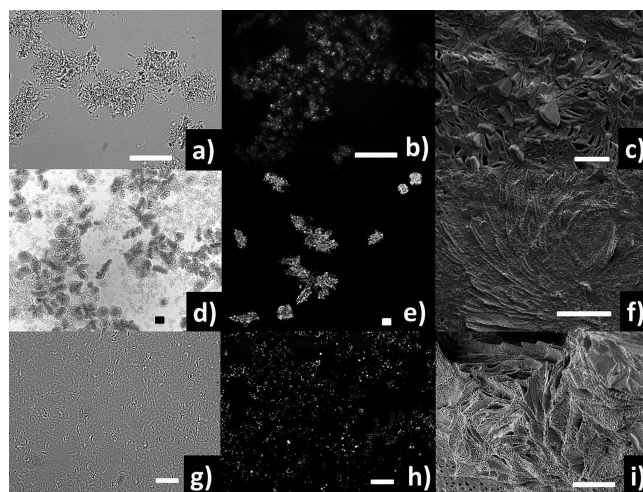


**Figure 2.** Optical microscopy (under normal and polarized light) and cryo-SEM images of gels of (a—c) BW; (d—f) FW, and (g—i) CLW. Scale bars = 50 $\mu$m (a, b, g, and h); 20 $\mu$m (d and e); 10 $\mu$m (f); and 1 $\mu$m (i and c).

with a comparatively higher crystalline weight fraction), the possibility of creating loose entanglements is higher. These entanglements can act as transient junction points, which can contribute to the elasticity but sustain only a very low magnitude of stress, as confirmed from amplitude and frequency sweeps discussed later in the text. The platelet-like crystals are clearly distinguishable in spherical crystalline aggregates of BW (Figure 2c), while flat crystals are seen radiating outward from the center to form spherical units in the case of FW (Figure 2f). Among the other four waxes, the most striking results were observed for the CLW gel, where the $G'$ at the crossover point was exceptionally high (~115 Pa), while the gelation occurred only after completion of the crystallization event, indicating that gel formation is a result of a significant reorganization of the crystalline phase at lower temperatures. As seen from Figure 2h and i, CLW crystallizes into very fine linear particles that are further organized into an open aggregate-like structure (Figure 2g). The sparse (noncompacted) packing is also evident from a low birefringence seen in the polarized light microscopy image (Figure 2h). The formation of such crystalline particles by CLW is attributed to a high proportion of linear hydrocarbons ($n$-alkanes).[42] The formation of gels with higher elasticity at lower crystalline mass

fraction is in agreement with previously reported studies on CLW-oil organogels.[16,20]

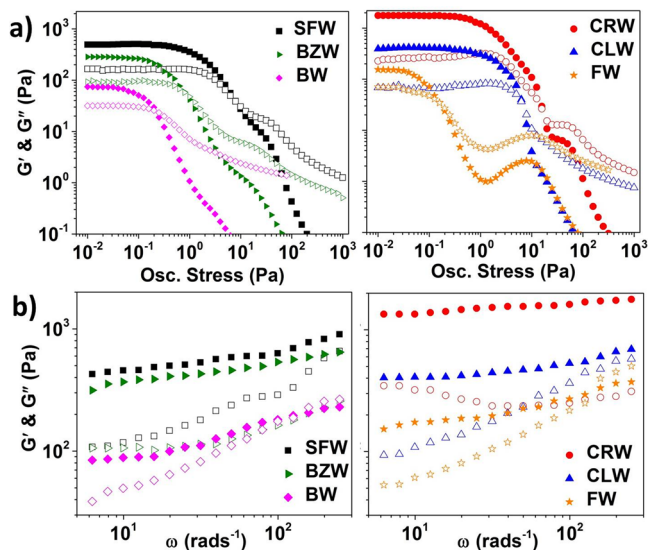The plots from oscillatory amplitude and frequency sweeps done on organogels are shown in Figure 3. As seen from the



**Figure 3.** (a and b) Amplitude (at $\nu = 1$ Hz) and frequency (at $\tau = 0.02$ Pa) sweeps for gels made at the $C_g$ of respective waxes. $G'$ and $G''$ are shown as filled and open symbols, respectively.

graphs, none of the studied samples satisfied the rheological definition of a "strong gel" ($G''/G'$ ($\omega$) $\leq 0.1$). However, the CRW gel did show the least frequency dependence (more or less linear curve in Figure 3b), higher $G'_{LVR}$ value, and higher oscillatory yield stress in comparison to other gels. As discussed earlier, the elasticity of BW and FW organogels is attributed to loose entanglements of large crystals, and because of this structure, the gels can sustain only a lower magnitude of stress, which is confirmed from low values of dynamic moduli in the linear response region. Moreover, these gels also showed very low values of $\tau^*$ (<0.05 Pa) and a narrow yield zone with $\tau_{dy}$ <0.25 Pa.

The yield zone or, more specifically, the slope of the curve in the yield zone gives information about the breakage of intermolecular forces holding up the structure. A narrow yield zone points at the fact that the structure breakdown occurs at once (all bonds break at the same force). The weak structure of BW and FW gels is further evident from a prominent crossover (tan $\delta = G''/G' > 1$) at higher $\omega$, which is a confirmation of structure breakdown at high rates of deformation. When comparing the gels made with waxes containing $hmc$, it can be seen that SFW gel was much softer than CRW and yielded at much lower force ($\tau_{dy} = 9.9$ Pa compared to 19.8 Pa for the CRW gel). However, it should be noted that SFW gel was formed at a $C_g$ of only 0.5%wt, whereas a high $C_g$ of 4%wt was required for CRW.

The differences in $C_g$ can be explained from the morphology of crystals formed in these two gels (Figure 4a–f). SFW crystals had an anisotropic, rod-like morphology (with lengths spanning the micrometer range), which is considered to be the most desirable shape of elementary assemblies (building blocks) to immobilize a large volume of solvent for efficient gelation.[35] The rod-like morphology of SFW is attributed to its high content (>95%wt) of wax esters, which are known to be the
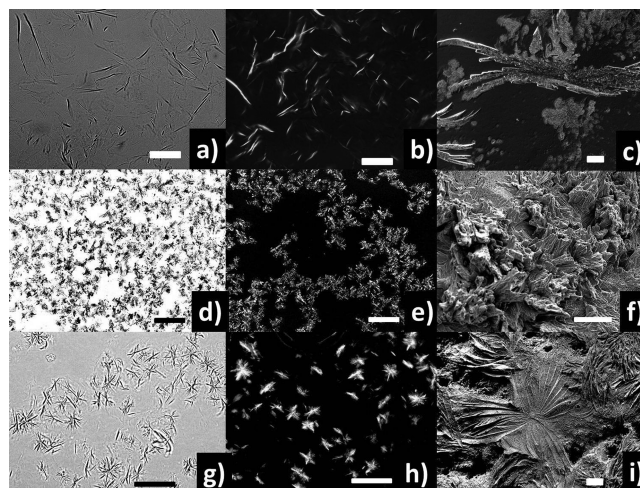


**Figure 4.** Optical microscopy (under normal and polarized light) and cryo-SEM images of gels of (a–c) SFW; (d–f) CRW; and (g–i) BZW. Scale bars = 50 $\mu$m (a, b, d, and e); 20 $\mu$m (g and h); 10 $\mu$m (c and f); and 1 $\mu$m (i).

main components responsible for excellent gelation behavior of most natural waxes.[14,15,25] Interestingly, in recently published work by Blake and Marangoni,[43] they have concluded based on cryo-SEM imaging that the morphology of SFW (along with other waxes such as CLW and rice bran wax) was "platelet-like", contrary to the observed morphology in the current work. In the case of CRW, the three-dimensional crystals of less than 10 $\mu$m in size are seen stacked closely together into larger aggregates (50–100 $\mu$m), and thus, a relatively higher crystalline mass fraction is required for gelation because the network formation is expected to be a result of the overlapping of spherical volumes of these aggregates. For waxes with $mmc$, both CLW and BZW gels showed similar frequency dependence, but the gel formed by BZW was comparatively more brittle and showed breakdown and yielding at lower stress values. The crystal morphology in the BZW gel was quite different from other waxes, showing a distinct "sea urchin"-like morphology (Figure 4i). Formation of such interestingly organized structures has been explained through crystal design and engineering and is attributed to a two-stage crystallization process initiated by a three-dimensional spherulite formation at the nucleation center followed by the organization of needle-like crystals in the outer layer, resulting in a radially oriented growth.[44,45] Such structures are also easily identifiable when viewed under an optical microscope (Figure 4g and h).

The yielding-type behavior with a strong shear thinning nature of all the gels is evident from the curves of apparent viscosity ($\eta_{app}$) versus shear rate ($\dot{\gamma}$) as shown in Figure 5b. Flow parameters such as apparent yield stress ($_{app}\tau_y$) and flow index ($n$) were calculated by fitting the data to a three-parameter model (Hershel Bulkley, eq 1).

$$\tau = {}_{app}\tau_y + K\dot{\gamma}^n \tag{1}$$

where $K$ = consistency coefficient and $\dot{\gamma}$ = shear rate.

The Hershel Bulkley model is one of the most commonly used models for characterizing materials that display non-Newtonian behavior after yielding, and the value of $n$ can be used as a measure to define the degree of shear thinning ($n < 1$) or shear thickening ($n > 1$) of the material. All the gel samples showed a prominent shear thinning flow behavior ($n < 1$), but the degree of shear thinning was highest for CRW gels, which
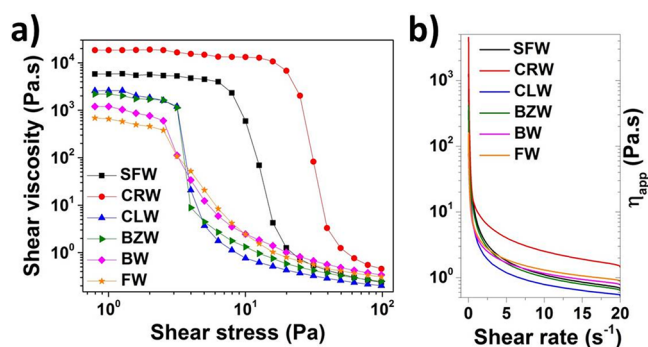
**Figure 5.** (a) Data from stress ramp shown as shear viscosity versus shear stress and (b) apparent viscosity ($\eta_{app}$) versus shear rate.

incidentally also had the highest $_{app}\tau_y$ (Table S2). In addition, the CRW gel also showed the highest static yield stress ($\tau_{sy}$) determined from the plots of the stress ramp (Figure 5a). The $\tau_{sy}$ measured using methods such as stress ramp and stress growth is defined as the minimum stress required for initiating flow, whereas the $_{app}\tau_y$ determined by model fitting is defined as the minimum stress required for maintaining flow and is often lower in values than the former.[37,46,47] The $\tau_{sy}$ and $_{app}\tau_y$ for all the gels were close to each other except for the CRW gel, where the $\tau_{sy}$ was almost 3 times larger than $_{app}\tau_y$. Such a big difference in stresses required for initiating and maintaining flow is taken as an indication of the existence of more than one structure that makes up the body of a material.[37,47] One of these structures is built up only during rest and can undergo breakdown under relatively lower shear, while a more robust structure that can withstand moderate shear rates contributes to the $_{app}\tau_y$.[46,47] Since $\tau_{sy}$ is a consequence of combined structures, it is expected to be higher than $_{app}\tau_y$. The high zero-shear viscosity of CRW gel (Figure 5b) confirms that the network structure is built up by overlapping spherical volumes of large aggregates, and a strong shear thinning behavior is a consequence of the disruption of aggregate clusters into smaller ones, which is driven by the mechanical energy. It is also important to note that although the yield stress values of these gels are rather low, they are still appreciably high to prevent gravitational settling of the particle network that structures the gels,[32] which was also confirmed from the absence of any phase separation in our samples stored for more than a month at 5 °C. Moreover, the stored samples were also periodically tested using oscillatory rheological measurements to evaluate any structure changes over 4 weeks of storage, and the results (Figure S4) confirm the stability of these gels.

Thixotropy has been defined in different ways by different authors over the years. While some authors refer to thixotropy simply as a time-dependent decrease in viscosity at a constant shear rate, other authors also include the reversible and gradual recovery of the consistency (which was lost on shearing) when the stress or shear rate is removed.[48−50] The term "gradual" when understood in terms of "finite time" required for structure recovery, makes the definition of thixotropy complete by enabling the inclusion of shear-thinning materials that show a rapid recovery (near zero time of recovery), which were previously known by the term "structural viscosity".[50] The word "reversible" could mean both a complete recovery (viscosity attains the original values or almost close to the original values on removal of shear) or a less desirable, partial recovery (flow-induced irreversible structural changes leading to an irreversible loss in viscosity on removal of shear). Thus, the thixotropic

behavior is best studied by tracking the material response resulting from stepwise changes in shear rate, as the coupled effect of time and shear rate can be clearly separated in such experiments.[51,52] A specific rheological test that is utilized to measure thixotropy is known as 3-ITT; it consists of three consecutive steps in control rate mode with alternating low and high shear rates.[36] The fraction of $\eta_{app}$ recovered in the third step or interval gives a measure of thixotropic recovery of the material.[22,53] The plots from 3-ITT done on organogels are shown in Figure S5. The thixotropic recovery for the gels were as follows: SFW (43.52%), CRW gel (15.84%), CLW (58.64%), BZW (67.34%), BW (80.77%), FW (56.52%). The CRW gel showed the least thixotropic recovery among the studied gels in spite of having a comparatively highest viscosity at rest as well as the highest $\tau_{sy}$ and $_{app}\tau_y$. Such behavior is usually associated with brittle gels that display a high gel strength and a narrow LVR as well as yield zone. However, from the results discussed in Figure 3, the CRW gel did not show a "brittle-type" failure, as confirmed from a broader yield zone, which indicates that the bonding in the network of crystalline particles is more heterogeneous, leading to a nonuniformity in bonding strength and consequent "ductile-type" failure.[54] This nonuniformity in the bonding strength is also evident from almost a 3-fold difference between $\tau_{sy}$ (~20.06 Pa) and $_{app}\tau_y$ (6.99 Pa), which basically tells us that 3 times higher force is required to initiate the flow compared to maintaining flow. The network structure in CRW can thus be assumed to be a random agglomeration of aggregated crystalline particles, and the local bonding strength among the aggregates may be stronger in certain regions compared to other regions due to localized crowding of aggregates. As the gel is sheared, with time, the structure breaks down into smaller clusters of aggregates that can contribute to the viscosity enhancement of the solvent, but the restructuring of these clusters into a coherent network is avoided because the Brownian motion is overcome by shear forces. In contrast, BW and BZW gels showed a reasonable thixotropic recovery (80.77% and 67.34%, respectively). From the microstructure studies, these two gels show spherical-type building units that are connected together into a network by a weak yet more uniform type of bonding (homogeneous bonding strength), and thus, all bonds can be broken down at the same applied force (supported well by narrow yield zone seen for these samples), resulting in a flow-induced structure breakdown that is non-time-dependent (linear curves in first and third interval of 3ITT, Figure S5). To further understand the structure of the sheared sample, mixed flow-oscillatory measurements were carried out on samples by first subjecting them to increasing shear rates from 0.01 to 20 s$^{-1}$ followed by frequency sweeps (0.01−10 Hz or 0.06−62.8 rads$^{-1}$). The graphs of shear moduli plotted as a function of angular frequency are shown in Figure 6. As seen from the figure, the quick recovery from flow-induced structure breakdown was seen only in BW and BZW samples ($G' > G''$ at $\omega_0$ = 0.06 rad s$^{-1}$), while the rest of the gels showed liquid-like behavior at low frequency. CRW gels, on the other hand, showed complete liquification, with a viscous component dominating over the entire frequency range. On comparing these curves with results from frequency sweeps done on unsheared samples, it can be seen that, out of the six waxes studied in this work, CRW showed a maximum loss of structure ($G'$ values showing more than 100-fold reduction after the flow step), while BW showed the least structure loss
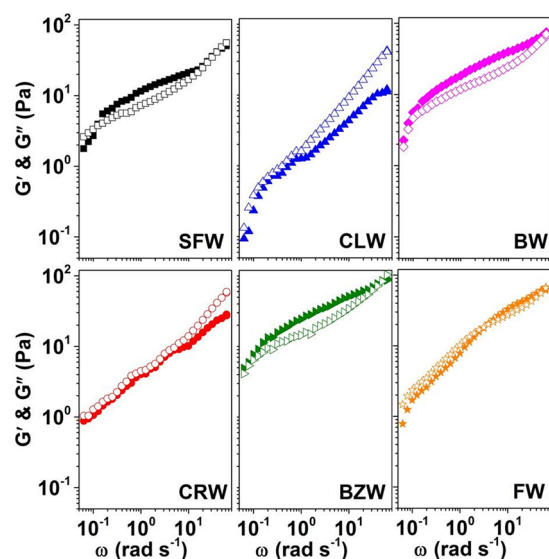
**Figure 6.** Data from frequency sweeps (from the flow-frequency tests) done on samples that were subjected to the flow test.

($G'$ values showing close to 2-fold reduction after the flow step), which is in agreement with 3ITT results.

To conclude, the rheological behavior of wax-based physical gels can be assumed to have characteristics of a flocculated suspension (at low volume fractions of colloidal particles) as well as a semidilute polymer solution. At a certain concentration, $C_g$ (analogous to $C^*$ in the case of a semidilute polymer solution), a 3D network or agglomeration of aggregated crystalline particles is created to form a viscoelastic gel, which might show "ductile-type" or "brittle-type" deformation under applied shear depending on the uniformity of bonding strength connecting the aggregated particles (as seen in a flocculated suspension). The $C_g$ and the rheological behavior are strongly influenced by the morphology of the primary crystalline particles as well as the subsequent aggregation of these primary particles, which, in turn, depends on the chemical components present in waxes. The waxes studied in this work are of natural origins, and thus, they can be used for potential applications in biorelated fields such as food, pharmaceutical, and cosmetics industries.[55] For instance, the gelling of edible oils at such low concentrations of waxes can be exploited in the formulation of food products with low saturated fat content. The information obtained through this work will help us in setting criteria for selecting waxes. For instance, it is not the melting range but the relative proportion of individual chemical constituents that determines the rheological properties of obtained gels. However, since these gels are rather "weak" in nature with high shear sensitivity and low thixotropic recovery, incorporation of high-melting fats will be necessary to obtain structured oil systems (i.e., hybrid systems) with desired properties for actual food applications.[56]

## ■ ASSOCIATED CONTENT

### Ⓢ Supporting Information

Chemical composition of waxes (Table S1); flow parameters of gels (Table S2); photograph of organogels (Figure S1); chemical structures of main wax components (Figure S2); plots of temperature ramps (Figure S3); graph of tan $\delta$ at v = 1 Hz measured at periodic intervals for all gels over a storage period of 1 month (Figure S4); and data from 3 ITT (Figure

S5). The Supporting Information is available free of charge on the ACS Publications website at DOI: 10.1021/acs.-jafc.5b01548.

## ■ AUTHOR INFORMATION

### Corresponding Author

*Tel: +32 (0) 9 264 6209. Fax: +32 (0) 9 264 6218. E-mail: Patel.Ashok@Ugent.be.

### Notes

The authors declare no competing financial interest.

## ■ REFERENCES

(1) Terech, P.; Weiss, R. G. Low molecular mass gelators of organic liquids and the properties of their gels. *Chem. Rev.* **1997**, *97*, 3133−3160.

(2) Weiss, R. G. The past, present, and future of molecular gels. What is the status of the field, and where is it going? *J. Am. Chem. Soc.* **2014**, *136*, 7519−7530.

(3) Terech, P.; Pasquier, D.; Bordas, V.; Rossat, C. Rheological properties and structural correlations in molecular organogels. *Langmuir* **2000**, *16*, 4485−4494.

(4) Bui, A.; Virgilio, N. Tuning organogel properties by controlling the organic-phase composition. *Ind. Eng. Chem. Res.* **2013**, *52*, 14185−14191.

(5) Wang, D.; Zhao, J.; Liu, X.; Sun, F.; Zhou, Y.; Teng, L.; Li, Y. Parenteral thermo-sensitive organogel for schizophrenia therapy, in vitro and in vivo evaluation. *Eur. J. Pharm. Sci.* **2014**, *60*, 40−48.

(6) Główka, E.; Wosicka-Frąckowiak, H.; Hyla, K.; Stefanowska, J.; Jastrzębska, K.; Klapiszewski, Ł.; Jesionowski, T.; Cal, K. Polymeric nanoparticles-embedded organogel for roxithromycin delivery to hair follicles. *Eur. J. Pharm. Biopharm.* **2014**, *88*, 75−84.

(7) Vintiloiu, A.; Leroux, J.-C. Organogels and their use in drug delivery - A review. *J. Controlled Release* **2008**, *125*, 179−192.

(8) Raut, S.; Bhadoriya, S. S.; Uplanchiwar, V.; Mishra, V.; Gahane, A.; Jain, S. K. Lecithin organogel: A unique micellar system for the delivery of bioactive agents in the treatment of skin aging. *Acta Pharm. Sin. B* **2012**, *2* (1), 8−15.

(9) Morales, M. E.; Gallardo, V.; Clarés, B.; García, M. B.; Ruiz, M. A. Study and description of hydrogels and organogels as vehicles for cosmetic active ingredients. *Int. J. Cosmet. Sci.* **2010**, *32* (4), 314−314.

(10) Puigmartí-Luis, J.; Laukhin, V.; Pérez del Pino, Á.; Vidal-Gancedo, J.; Rovira, C.; Laukhina, E.; Amabilino, D. B. Supramolecular conducting nanowires from organogels. *Angew. Chem., Int. Ed.* **2007**, *46* (1−2), 238−241.

(11) Hughes, N. E.; Marangoni, A. G.; Wright, A. J.; Rogers, M. A.; Rush, J. W. E. Potential food applications of edible oil organogels. *Trends Food Sci. Technol.* **2009**, *20* (10), 470−480.

(12) Pernetti, M.; van Malssen, K. F.; Flöter, E.; Bot, A. Structuring of edible oils by alternatives to crystalline fat. *Curr. Opin. Colloid Interface Sci.* **2007**, *12* (4−5), 221−231.

(13) Marangoni, A. G.; Garti, N. *Edible Oleogels: Structure and Health Implications*; AOCS Press: Urbana, IL, 2011.

(14) Blake, A.; Co, E.; Marangoni, A. Structure and physical properties of plant wax crystal networks and their relationship to oil binding capacity. *J. Am. Oil Chem. Soc.* **2014**, *91* (6), 885−903.

(15) Hwang, H.-S.; Kim, S.; Singh, M.; Winkler-Moser, J.; Liu, S. Organogel formation of soybean oil with waxes. *J. Am. Oil Chem. Soc.* **2012**, *89* (4), 639−647.

(16) Toro-Vazquez, J. F.; Morales-Rueda, J.; Torres-Martínez, A.; Charó-Alonso, M. A.; Mallia, V. A.; Weiss, R. G. Cooling rate effects on the microstructure, solid content, and rheological properties of organogels of amides derived from stearic and (R)-12-hydroxystearic acid in vegetable oil. *Langmuir* **2013**, *29* (25), 7642−7654.

(17) Dassanayake, L. S. K.; Kodali, D. R.; Ueno, S. Formation of oleogels based on edible lipid materials. *Curr. Opin. Colloid Interface Sci.* **2011**, *16* (5), 432−439.

(18) Parish, E. J.; Shengrong, L.; Bell, A. D. Chemistry of waxes and sterols. In *Food Lipids: Chemistry, Nutirtion and Biotechnology*; Akoh, C. C., Min, D. B., Eds.; CRC Press: Boca Raton, FL, USA, 2000; pp 99−123.

(19) Patel, A. R.; Schatteman, D.; Vos, W. H. D.; Dewettinck, K. Shellac as a natural material to structure a liquid oil-based thermo reversible soft matter system. *RSC Adv.* **2013**, *3*, 5324−5327.

(20) Toro-Vazquez, J. F.; Morales-Rueda, J. A.; Dibildox-Alvarado, E.; Charó-Alonso, M.; Alonzo-Macias, M.; González-Chávez, M. M. Thermal and textural properties of organogels developed by candelilla wax in safflower oil. *J. Am. Oil Chem. Soc.* **2007**, *84*, 989−1000.

(21) Patel, A. R.; Rajarethinem, P. S.; Gredowska, A.; Turhan, O.; Lesaffer, A.; De Vos, W. H.; Van de Walle, D.; Dewettinck, K. Edible applications of shellac oleogels: spreads, chocolate paste and cakes. *Food Function* **2014**, *5*, 645−652.

(22) Patel, A. R.; Schatteman, D.; De Vos, W. H.; Lesaffer, A.; Dewettinck, K. Preparation and rheological characterization of shellac oleogels and oleogel-based emulsions. *J. Colloid Interface Sci.* **2013**, *411*, 114−121.

(23) Hwang, H.-S.; Singh, M.; Bakota, E.; Winkler-Moser, J.; Kim, S.; Liu, S. Margarine from organogels of plant wax and soybean oil. *J. Am. Oil Chem. Soc.* **2013**, *90*, 1705−1712.

(24) Jana, S.; Martini, S. Effect of high-Intensity ultrasound and cooling rate on the crystallization behavior of beeswax in edible oils. *J. Agric. Food Chem.* **2014**, *62*, 10192−10202.

(25) Dassanayake, L. S. K.; Kodali, D. R.; Ueno, S.; Sato, K. Crystallization kinetics of organogels prepared by rice bran wax and vegetable oils. *J. Oleo Sci.* **2012**, *61*, 1−9.

(26) Alvarez-Mitre, F. M.; Toro-Vázquez, J. F.; Moscosa-Santillán, M. Shear rate and cooling modeling for the study of candelilla wax organogels' rheological properties. *J. Food Eng.* **2013**, *119*, 611−618.

(27) Alvarez-Mitre, F. M.; Morales-Rueda, J. A.; Dibildox-Alvarado, E.; Charó-Alonso, M. A.; Toro-Vazquez, J. F. Shearing as a variable to engineer the rheology of candelilla wax organogels. *Food Res. Int.* **2012**, *49*, 580−587.

(28) Morales-Rueda, J.; Dibildox-Alvarado, E.; Charó-Alonso, M.; Toro-Vazquez, J. Rheological properties of candelilla wax and dotriacontane organogels measured with a true-gap system. *J. Am. Oil Chem. Soc.* **2009**, *86*, 765−772.

(29) Pieter, W. Fractal particle gels in foods. In *Supramolecular and Colloidal Structures in Biomaterials and Biosubstrates*; Lal, M., Lillford, P. J., Naik, V. M., Prakash, V., Eds.; Imperal College Press and the Royal Society: London, UK, 2000; pp 157−173.

(30) Johansson, D. Weak gels of fat crystals in oils at low temperatures and their fractal nature. *J. Am. Oil Chem. Soc.* **1995**, *72*, 1235−1237.

(31) Visintin, R. F. G.; Lapasin, R.; Vignati, E.; D'Antona, P.; Lockhart, T. P. Rheological behavior and structural interpretation of waxy crude oil gels. *Langmuir* **2005**, *21*, 6240−6249.

(32) Emanuele, V.; Roberto, P.; Ruben, F. G. V.; Romano, L.; Paolo, D. A.; Thomas, P. L. Wax crystallization and aggregation in a model crude oil. *J. Phys.: Condens. Matter* **2005**, *17*, S3651.

(33) *Rheology: Concepts, Methods and Applications*; Chemtech Publishing: Toronto, Canada, 2006.

(34) Menard, K. P. *Dynamic Mechanical Analysis*; CRC Press: Boca Raton, FL, USA, 2008.

(35) Mewis, J.; Wagner, N. *Colloidal Suspension Rheology*; Cambridge University Press: Cambridge, UK, 2012.

(36) Mezger, T. G. *The Rheology Handbook: For Users of Rotational and Oscillatory Rheometers*; Vincentz Network GmbH & Co. KG: Hannover, Germany, 2006.

(37) Cheng, D. C. H. Yield stress: A time-dependent property and how to measure it. *Rheol. Acta* **1986**, *25*, 542−554.

(38) Wang, Y.; Tang, L.; Yu, J. Investigation of spontaneous transition from low-molecular-weight hydrogel into macroscopic crystals. *Cryst. Growth Des.* **2008**, *8*, 884−889.

(39) Houton, K. A.; Morris, K. L.; Chen, L.; Schmidtmann, M.; Jones, J. T. A.; Serpell, L. C.; Lloyd, G. O.; Adams, D. J. On crystal versus fiber formation in dipeptide hydrogelator systems. *Langmuir* **2012**, *28*, 9797−9806.

(40) Morris, K. L.; Chen, L.; Raeburn, J.; Sellick, O. R.; Cotanda, P.; Paul, A.; Griffiths, P. C.; King, S. M.; O'Reilly, R. K.; Serpell, L. C.; Adams, D. J. Chemically programmed self-sorting of gelator networks. *Nat. Commun.* **2013**, *4*, 1480.

(41) Gennes, P. G. D. *Scaling Concepts in Polymer Physics*; Cornell University Press: Ithaca, NY, 1979.

(42) Toro-Vazquez, J.; Morales-Rueda, J.; Mallia, V. A.; Weiss, R. Relationship between molecular structure and thermo-mechanical properties of candelilla wax and amides derived from (R)-12-hydroxystearic acid as gelators of safflower oil. *Food Biophys.* **2010**, *5*, 193−202.

(43) Blake, A. I.; Marangoni, A. G. Plant wax crystals display platelet-like morphology. *Food Struct.* **2015**, *3*, 30−34.

(44) Heijna, M. C. R.; Theelen, M. J.; van Enckevort, W. J. P.; Vlieg, E. Spherulitic growth of hen egg-white lysozyme crystals. *J. Phys. Chem. B* **2007**, *111*, 1567−1573.

(45) Ueno, S.; Nishida, T.; Sato, K. Synchrotron radiation microbeam X-ray analysis of microstructures and the polymorphic transformation of spherulite crystals of trilaurin. *Cryst. Growth Des.* **2008**, *8*, 751−754.

(46) Galindo-Rosales, F. J.; Rubio-Hernandez, F. J. Static and dynamic yield stresses of Aerosil® 200 suspensions in polypropylene glycol. *Appl. Rheol.* **2010**, *20*, 22787.

(47) Galindo-Rosales, F. J.; Rubio-Hernández, F. J.; Velázquez-Navarro, J. F.; Gómez-Merino, A. I. Structural level of silica-fumed aqueous suspensions. *J. Am. Ceram. Soc.* **2007**, *90*, 1641−1643.

(48) Mewis, J. Thixotropy - A general review. *J. Non-Newtonian Fluid Mech.* **1979**, *6*, 1−20.

(49) Mewis, J.; Wagner, N. J. Thixotropy. *Adv. Colloid Interface Sci.* **2009**, *147−148*, 214−227.

(50) Barnes, H. A. Thixotropy - A review. *J. Non-Newtonian Fluid Mech.* **1997**, *70*, 1−33.

(51) Weltmann, R. N. Breakdown of thixotropic structure as function of time. *J. Appl. Phys.* **1943**, *14*, 343−350.

(52) Coussot, P.; Nguyen, Q. D.; Huynh, H. T.; Bonn, D. Viscosity bifurcation in thixotropic, yielding fluids. *J. Rheol.* **2002**, *46*, 573−589.

(53) Patel, A. R.; Schatteman, D.; Lesaffer, A.; Dewettinck, K. A foam-templated approach for fabricating organogels using a water-soluble polymer. *RSC Adv.* **2013**, *3*, 22900−22903.

(54) Uhlherr, P. H. T.; Guo, J.; Tiu, C.; Zhang, X. M.; Zhou, J. Z. Q.; Fang, T. N. The shear-induced solid−liquid transition in yield stress materials with chemically different structures. *J. Non-Newtonian Fluid Mech.* **2005**, *125*, 101−119.

(55) Doan, C. D.; Van de Walle, D.; Dewettinck, K.; Patel, A. R. Evaluating the oil-gelling properties of natural waxes in rice bran oil: rheological, thermal, and microstructural study. *J. Am. Oil Chem. Soc.* **2015**, DOI: 10.1007/s11746-015-2645-0.

(56) Patel, A. R.; Dewettinck, K. Comparative evaluation of structured oil systems: shellac oleogel, HPMC oleogel and HIPE gel. *Eur. J. Lipid Sci. Technol.* **2015**, DOI: 10.1002/ejlt.201400553.